



Contents lists available at ScienceDirect

Environmental Pollution

journal homepage: www.elsevier.com/locate/envpol

Ultra-rapid catalytic degradation of 4-nitrophenol with ionic liquid recoverable and reusable ibuprofen derived silver nanoparticles[☆]

Syeda Sara Hassan^{a, b, c, *}, Krista Carlson^b, Swomitra Kumar Mohanty^{b, c}, Sirajuddin^d, Ali Canlier^{e, f}

^a US.-Pakistan Center for Advanced Studies in Water (USPCASW), Mehran University of Engineering & Technology (MUET), Jamshoro, Sindh, 76062, Pakistan

^b Department of Metallurgical Engineering, University of Utah, 201 Presidents Circle, Salt Lake City, UT 84112, USA

^c Department of Chemical Engineering, University of Utah, 201 Presidents Circle, Salt Lake City, UT 84112, USA

^d National Centre of Excellence in Analytical Chemistry, University of Sindh, Jamshoro, Sindh Pakistan

^e Department of Chemical Engineering and Applied Chemistry, College of Engineering, Chungnam National University, Daejeon 34134, South Korea

^f Department of Materials Science and Nanotechnology Engineering, Abdullah Gul University, Kayseri 38080, Turkey

ARTICLE INFO

Article history:

Received 21 June 2017

Received in revised form

22 October 2017

Accepted 29 October 2017

Available online xxx

Keywords:

Silver nanoparticles

Ibuprofen analgesic

4-Nitrophenol

Ionic liquid

Recycle

ABSTRACT

This study reports a one-pot and eco-friendly method for the synthesis of spherical ibuprofen derived silver nanoparticles (IBU-AgNPs) in aqueous media using ibuprofen analgesics drug as capping as well as reducing agent. Formation of AgNPs occurred within a few min (less than 5 min) at room temperature without resorting to any harsh conditions and hazardous organic solvents. Synthesized AgNPs were characterized with common analytical techniques. Transmission electron microscope (TEM) images confirmed the formation of spherical particles having a size distribution in the range of 12.5 ± 1.5 nm. Employment of IBU analgesic aided the control of better size distribution and prevented agglomeration of particles. Such AgNPs solution was highly stable for more than two months when stored at ambient temperature. The IBU-AgNPs solution showed excellent ultra-rapid catalytic activity for the complete degradation of toxic 4-nitrophenol (4-NPh) into non-toxic 4-aminophenol (4-APh) within 40 s. AgNPs were recovered with the help of water insoluble-room temperature ionic liquid and reused with enhanced catalytic potential. This method provides a novel, rapid and economical alternative for the treatment of toxic organic pollutants to maintain water quality and environmental safety against water pollution. It is extendable for the control of other reducible contaminants in water as well. Furthermore, this catalytic activity for an effective degradation of organic toxins is expected to play a crucial role for achieving the Sustainable Development Goal 6 set by United Nations.

© 2017 Elsevier Ltd. All rights reserved.

1. Introduction

Noble metal nanoparticles (NPs) have been widely used for catalytic degradation in recent years (Hassan et al., 2011; Kalwar et al., 2013; Kästner and Thünemann, 2016; Gong and Mullins, 2009; Chimentao et al., 2004; Kannan and John, 2009; Kalwar et al., 2014) due to their changed morphology which provides large surface area and surface free energy resulting from reduction

in size. Among the different noble NPs, nano-sized silver is particularly attractive for catalytic degradation due to its high surface area to volume ratio as compared to other noble metals (Tsujino and Matsumura, 2005; Salam et al., 2014; Sasidharan et al., 2015). Silver nanostructures in different shapes such as NPs, nanowires, nanocubes, nanodisks and nanoprisms offer potential applications for various emerging research areas including antimicrobial activity, imaging, biomedicine, optics, catalysis and surface enhanced Raman spectroscopy (SERS) detection (Yamamoto et al., 2006; Kim and Lee, 2010; Zhang et al., 2010; Netzer et al., 2009; Tang et al., 2008; Halvorson and Vikesland, 2010; Wang et al., 2011; Bryaskova et al., 2010). Compared with other noble metals (e.g., gold, platinum, palladium), silver is less expensive and has good physical and chemical properties.

Industrial effluents contain many hazardous substances such as

[☆] This paper has been recommended for acceptance by Baoshan Xing.

* Corresponding author. Environment Engineering Department, US.-Pakistan Center for Advanced Studies in Water (USPCASW), Mehran University of Engineering & Technology (MUET), Jamshoro, Sindh, 76062, Pakistan. Tel.: +92 22 7711226.

E-mail address: ssarahassan@gmail.com (S.S. Hassan).

heavy metals, organic and inorganic pollutants that are discharged from industrial process through water sources and potentially lead to detrimental health effects. Aromatic nitro compounds cause adverse effects in the environment and threaten wellbeing of humans as well as animals. For the removal of these compounds, a variety of traditional methods are reported for degradation and detoxification treatments, e.g. coagulation, ozonation, biological treatment and adsorption. However, these methods require extended times for the completion of reaction between substrates, and expensive procedures due to use of chemicals and solvents. Inefficient treatment, secondary pollution and increased cost due to additional removal processes are other disadvantages to count a few. To avoid these circumstances, using advanced oxidation techniques exploiting nanomaterials is an alternative, cost-effective, fast and proper method for degradation of aromatic nitro compounds such as nitrobenzene or 4-nitrophenol (4-NPh). These nitro compounds are mostly used for industrial, agricultural and defense objectives and they impose detrimental health effects as they are carcinogenic (Uberoi and Bhattacharya, 1997).

4-NPh is an organic pollutant which is mostly discharged by chemical industries dealing with pesticides, dyes, pharmaceuticals and rubber. Therefore, it is commonly released and has serious impact on the environment (Kiasat and Davarpanah, 2013; Mustafa et al., 2011; Uberoi and Bhattacharya, 1997). According to the US-Environmental Protection Agency (EPA), the permissible limit for 2, 4-di-NPh, 2-NPh and 4-NPh are 10 ng/L in natural waters, which reflects the extreme nature of these toxic organic pollutants (Poddeh et al., 1995).

Recently, many scientists have focused on the removal of toxic organic pollutants using noble metal nanostructures (NSs) including gold NPs bound with starch and ibuprofen (Chairam et al., 2017; Hassan et al., 2012, 2015), silver NPs mediated with cefditorene (Junejo et al., 2013), noble metal nanomaterials (Au, Ag and Pt) stabilized with varying substances. They demonstrated that these materials perform highly favorable catalytic and sensing activities within environmental applications (Luo et al., 2014; Dou et al., 2014; Tagar et al., 2011). Amino acid derived nickel NPs (Khaskheli et al., 2016), mercury nanoparticles (Tagar et al., 2012), core-shell nanoparticles have been used successfully for reduction of 4-nitrophenol and hydrodechlorination of 4-chlorophenol (Dong et al., 2015). Magnetic Pd/Ni NPs catalyst supported by N-doped mesoporous carbon have been derived from nickel metal organic framework (Ni MOF) for hydrodechlorination of 4-chlorophenol (Cui et al., 2016) and so forth. Stability of noble NPs is the key issue as their catalytic activity has potential to show superior effectiveness due to their size and geometry which results in an effect of large surface area to volume ratio. Metal NPs, in particular AgNPs, have been prepared by various methods such as sonochemical synthesis (Aksomaityte et al., 2013), hydrothermal synthesis (Darroudi et al., 2012), electron beam irradiations (Kim et al., 2012) which use diverse capping/reducing agents such as Cefditorene (Junejo et al., 2013), 3, 4- ethylenedioxythiophene (Balamurugan et al., 2009), leave and seed extractions (Kouvaris et al., 2012; Jagtap and Bapat, 2013; Bar et al., 2009) and so on.

The present study has focused on the rapid fabrication of a homogenous AgNPs sol with the use of ibuprofen analgesic as a highly efficient and effective capping and reducing agent. Achieving long term stability of AgNPs as well as ultra-fast reaction rate for efficient degradation of 4-nitrophenol (toxic) to 4-aminophenol (non-toxic) are main goals of the work. In our previous report we used ibuprofen as reducing and capping agents but there is significant difference between our present and previous protocols. The present study avoids the use of NaOH (pH set to 6.31) at no heating and prevents abrupt formation of AgNPs, whereas previous method used NaOH (pH, 7.50) with heating at 85 °C for 4 min.

Current AgNPs have been synthesized within a few seconds reaction at room temperature without any harsh conditions (temperature, pressure, etc.). This method depends on the reduction of silver nitrate with soluble ibuprofen drug. The ultra-fast catalytic degradation by IBU-AgNPs was demonstrated on 4-NPh, a common organic pollutant found in aqueous industrial waste samples. This process is highly favorable on account of being based on an eco-friendly, facile and rapid synthesis of a homogenous catalyst (IBU-AgNPs), requiring short time of reactions and product formation, and having the advantages of reusability and easy recovery of the catalyst.

2. Materials and methods

2.1. Chemicals and reagents

Silver nitrate (AgNO₃, 99%), ibuprofen (C₁₃H₁₈O₂, 99%), sodium borohydride (NaBH₄, 98%), 4-Nitrophenol (O₂NC₆H₄OH, 99.5%), methanol (CH₃OH, 99.8%) and hydrochloric acid (HCl, 99.999%) were purchased from Sigma Aldrich, Alfa Aesar and Fluka. and used as received. All stock solutions were prepared with de-ionized water of Milli-Q[®] except for the 0.5% ibuprofen standard solution which was prepared with methanol.

2.2. Instrumentation

Highly stable, spherical and well dispersed IBU-AgNPs were characterized by using Ultraviolet-visible (UV-Vis) spectroscopy, Fourier transform infrared (FTIR) spectroscopy, X-ray diffraction (XRD), TEM, zeta-potential (ZP) analyzer and differential light scattering (DLS) methods.

Aqueous solution samples containing AgNPs were firstly investigated by UV-Vis (Shimadzu UV-1800) spectrophotometer to determine the absorbance within 300–800 nm region.

FTIR spectra were recorded on Thermo Scientific Nicolet-6700, fixed with a deuterated triglycine sulfate (DTGS) detector. The spectrum software version 6.3.5 (Perkin Elmer, Inc.) was used for data acquisition and instrument control. FTIR spectra were collected by incorporating the dried sample of IBU-AgNPs and ibuprofen drug in solid state KBr disc. Mid IR region (4000–400 cm⁻¹) was used with 32 scans and a resolution of 4 cm⁻¹.

Crystalline patterns were recorded on an XRD (Rigaku, Smart Lab) equipped with a CuK-alpha radiation source producing 1.5406 nm waves and operated at 40 kV and 15 mA for powder mode.

TEM images were recorded on a JEOL USA, JEM-1400 Plus-TEM scope instrument operated at 120 kV. TEM samples of synthesized IBU-AgNPs were prepared on amorphous carbon-coated copper grids.

Zeta potential analyses have been carried out for monitoring nanoparticle stability or aggregation phenomenon in dispersion. Analyses were performed on a version 3.12 zeta potential analyzer of Brookhaven Instruments Corporation (Holtville, NY) which uses phase analysis light scattering (PALS).

2.3. Procedure for sample preparation

2.3.1. Synthesis of IBU-AgNPs sol

Synthesis of highly stable, spherical and well dispersed AgNPs sol was performed with a chemical reduction method which makes use of ibuprofen drug. First of all, stock solutions of AgNO₃ (0.5% in Milli-Q[®] water) and Ibuprofen (0.5% in methanol) were prepared. In a typical synthesis, we took a 100 μL of AgNO₃ solution and added it into a 10 mL test tube which is followed by addition of 100 μL of ibuprofen solution. The final volume was adjusted to 10 mL by

addition of Milli-Q[®] water. The solution was shaken vigorously until its color turned from colorless to transparent bright yellow of a colloidal form at room temperature, which points out nearly complete conversions of silver ions into nanoparticles. Final pH of solutions revealed to be in the range of 6.31 ± 0.1 . Formation of AgNPs was completed within a few min (less than 5 min) of reaction in the test tube without need to apply any harsh conditions (temperature, pressure and so on). The resulting solution was analyzed by a UV-visible spectrometer in the range of 300–800 nm in order to observe the surface plasmon resonance band around 392 nm which is clear evidence to the formation of the desired AgNPs sol.

2.3.2. Sample preparation for FTIR and XRD analyses

Bright yellow colloidal solution of AgNPs was transferred onto petri dishes and heated at 100 °C on a water bath equipped with a temperature control system until solvent evaporation is complete. The product was cooled and washed several times with de-ionized water and ethanol in order to eliminate any untreated species of ibuprofen. AgNPs was then ultra-centrifuged at 14,000 rpm after suspending in water again. After washing, the product was dried in an oven at 100 °C for at least 1 h. Dried black particles accumulated on the petri dish were scraped with a clean glass slide and then transferred and stored in a separate small-size glass vial for FTIR and XRD analyses.

2.3.3. Sample preparation for TEM analysis

The size and morphology of the AgNPs was characterized by TEM (Jeol, USA). TEM was operating at an accelerating voltage of 120 kV. Ag nanoparticles were diluted with distilled water at 1:10 ratio, and an aliquot of 20 μ L was loaded onto amorphous carbon coated copper grids. The solution was left that way for 1 min and the excess was removed from the grid by blotting with a filter paper. The grids were placed in their grid box for 2 h to dry before imaging.

2.3.4. Sample preparation for zeta potential analyzer

Zeta PALS (phase analysis light scattering) potential analyzer was used for detection of the features of stability, charge and size of nanoparticles. Optimized values for parameters of wavelength, field frequency, voltage, electrical field, sample count rate and reference count rate were set to 677 nm, 2.00 Hz, 4.00 V, 10.66 V/cm, 31 kcps and 893 kcps, respectively. As synthesized samples were diluted with a ratio of 5 mL of NPs sol to 50 mL of double-distilled water at pH = 6.31 for the measurement of zeta potential. Samples of AgNPs sol were shaken for 30 min prior to measurement of zeta potential.

2.3.5. Homogenous catalytic activity of IBU-AgNPs sol for the reduction of 4-NPh into 4-APh

In order to investigate the catalytic activity of synthesized AgNPs in a homogenous phase; stock solutions of 4-NPh and NaBH₄ were prepared at 0.001M and 1M concentrations, respectively, by dissolving in de-ionized water of Milli-Q[®]. Reactions of catalytic activity were carried out in an aqueous media placed in a standard quartz cell with 1 cm path length. We took 0.67 mL from 0.001 M 4-NPh solution and loaded into the cell, and then added 0.33 mL of 1 M NaBH₄ solution which is finally followed by addition of 100 μ L (0.1 mL) of AgNPs sol so that a final volume of 3.5 mL (pH = 6.31 ± 0.1) was reached. UV-visible spectra were recorded against a blank cell just 40 s later than the addition of AgNPs sol to the reaction cell. Faster scan rate of 1920 nm min⁻¹ was used to monitor the reaction at smallest possible interval.

2.3.6. Recovery and reuse of IBU-AgNPs sol

Metal nanoparticles can be recovered with the use of several

kinds of ionic liquids as reported in previous studies (Manojkumar et al., 2016; Hassan et al., 2011). In this study, 1-butyl-3-methylimidazolium hexafluorophosphate [BMIM-PF₆], a water insoluble ionic liquid (IL) at room temperature (Hassan et al., 2011), was used for the recovery of IBU-AgNPs sol. 150 μ L of IL [BMIM-PF₆] was inserted into a solution mixture of 4-NPh solution treated with AgNPs, and the mixture was shaken vigorously. As a result of shaking, AgNPs gathered on the surface of IL on the top of the solution as a noticeable blackish blot. This blot of AgNPs was separated from the mixture by pouring the supernatant. Saved AgNPs were washed 3 times with de-ionized water of Milli-Q[®] and were used repeatedly through this process for catalytic degradation of 4-NPh (toxic) into 4-APh (non-toxic), which is a common organic pollutant present in waste water.

3. Results and discussion

3.1. UV-visible spectroscopy

Throughout the synthesis of ibuprofen derived AgNPs, all concentrations were fixed at 0.5% for AgNO₃ and at 0.5% for IBU as mentioned above. AgNO₃ source was dissolved in de-ionized water and the silver ions Ag (I) were produced thereby. Free metallic silver (Ag⁰) atoms were produced at the initial state of the reduction of Ag (I) ions, and they successively grow into crystalline AgNPs within a few min. This process takes place at ambient temperature without using any hazardous solvents and chemicals as shown in Scheme 1. Besides acting as a reducing agent, ibuprofen played the role of a capping/stabilizing agent so as to prevent AgNPs from absorbing other constituents of the mixture or interacting through each other's surface, thus the agglomeration of metal NPs were avoided.

Fig. 1 shows the UV-visible absorption spectra of synthesized IBU capped AgNPs at a wavelength (λ) range of 300–800 nm. It is seen that surface plasmon resonance (SPR) peaks shifted towards lower wavelength (blue region) at 392 nm due to a decrease in size of AgNPs.

3.2. FTIR spectroscopy

Fig. 2 shows the FTIR spectrum of AgNPs formed without heating and stirring of the solution during synthesis process. FTIR band at 2773 cm⁻¹ arises from C–H stretching of aromatic compound. The peak at 1627 cm⁻¹ indicates the asymmetric stretching of COO⁻ group. As compared to 1720 cm⁻¹ peak of pure ibuprofen (Meynen et al., 2009; Tagar et al., 2011), there is a large downward shift in analogous peak of ibuprofen derived AgNPs which verifies the strong interaction of ibuprofen with AgNPs (Junejo et al., 2014; Tagar et al., 2011; Tagar et al., 2012).

In this work, the peak at 1130 cm⁻¹ characterizes the –CO stretching for –COOAgNPs side of ibuprofen as evidenced by similar –CO stretching at 1056 and 1083 cm⁻¹ for –COOAuNPs and –COOAgNPs, which employ the same drug as capping agent (Hassan et al., 2015; Tagar et al., 2012). All of these observations fortified our conclusions that AgNPs formed with ibuprofen are capped and stabilized via –COO linkage as evidenced for other works of –COOAuNPs, –COOAuNSs and –COOHgNPs using the same drug (Hassan et al., 2012, 2015; Tagar et al., 2012). In our study, the peaks at 1495 and 1775 cm⁻¹ disappeared completely showing the absence of aromaticity and carbonyl characteristics.



Scheme 1. Proposed mechanism of ibuprofen capped silver nanoparticles.

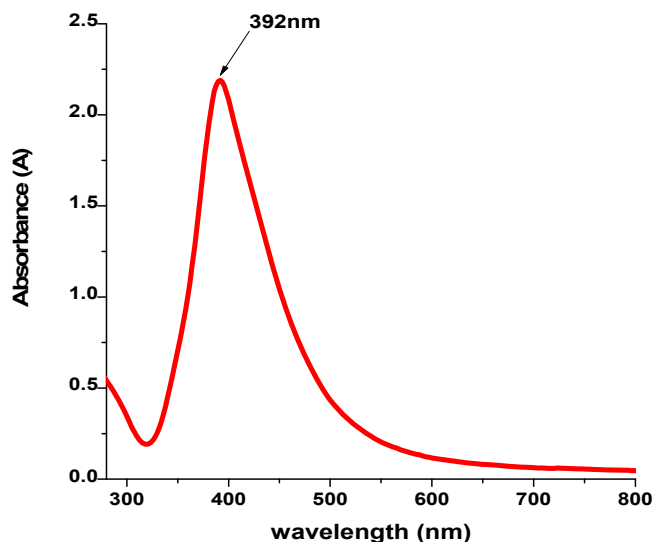


Fig. 1. UV-visible spectra of ibuprofen capped silver nanoparticles.

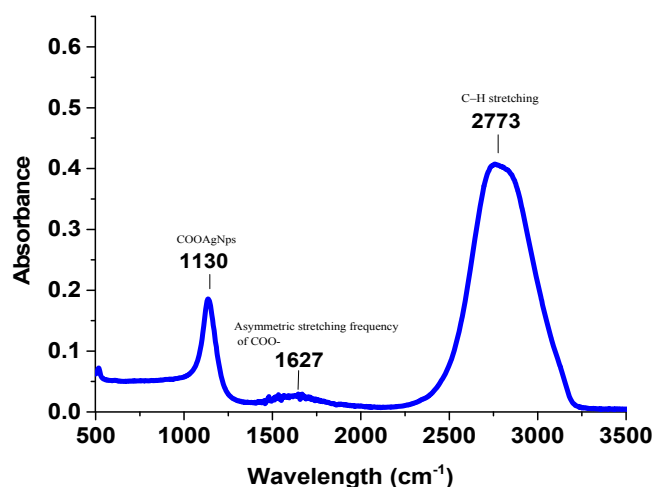


Fig. 2. FTIR spectra of ibuprofen capped silver nanoparticles.

3.3. X-ray diffraction

The crystalline patterns of AgNPs were determined by X-ray diffraction is shown in Fig. 3. Well-defined two theta values were observed at $2\theta = 38.6^\circ, 40.3^\circ, 63.3^\circ$ and 76.5° , which correspond to the four pronounced planes of diffraction miller indices (111), (200), (220) and (311), that are assigned to the face centered cubic crystal structure of AgNPs (Philip et al., 2011; Prakash et al., 2013; Peng et al., 2013; Safdar et al., 2015). XRD patterns clearly indicated that AgNPs are in crystalline structure and the average crystalline size was calculated using Debye-Scherrer formula (Klug and Alexander, 1974). The average diameter was found out to be approximately equal to the value found in TEM analysis.

3.4. Transmission electron microscopy

The particle size distribution and morphology of AgNPs were examined by TEM method. TEM images of AgNPs at different magnification are displayed in Fig. 4. Spherical formation of nanoparticles and narrow size distribution can be confirmed well from the images.

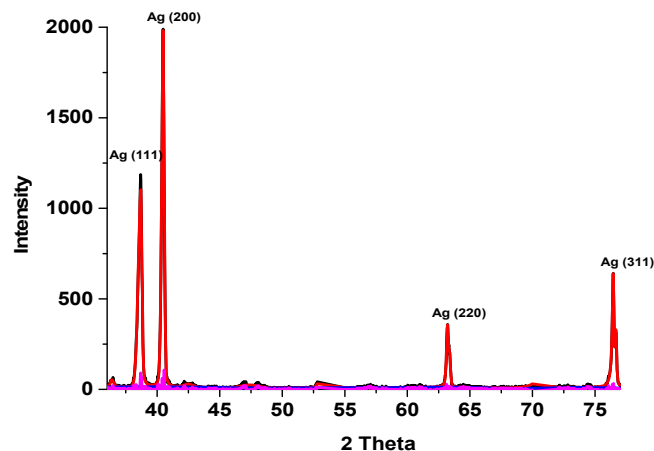


Fig. 3. XRD pattern of ibuprofen capped silver nanoparticles.

Particle size histogram was drawn out and average AgNPs diameter was calculated from the images by using ImageJ software (National Institutes of Health, USA). Average size of the most frequent type of particles was 12.5 ± 2 nm and particle size distribution ranged between 12.5 and 20 nm is shown in Fig. 5.

Silver nanoparticles synthesized with ibuprofen are spherical in shape with a smooth surface morphology likely because the interaction between surface silver atoms and functional groups of ibuprofen molecules is strong, and hence their capping ability is superb. Ibuprofen acts as both stabilizing and reducing agent in slightly acidic medium, and thus prevents the agglomeration of nanoparticles. Well dispersed spherical NPs with such small size may act as a nano-reactor/catalyst in homogeneous sol state and demonstrate potential catalytic activity for degradation of toxic pollutants (Stevanovic et al., 2012; Levin et al., 2008).

3.5. Zeta-potential and dynamic light scattering analyses

Zeta potential (ζ) is a physical property of nanomaterials, which is determined through the surface charge on nanoparticles in solution (colloids) (Safdar et al., 2015; Lin et al., 2010). Development of agglomerates depends on the surface charge that designates the stability of dispersed NPs. Reasonable magnitude of surface charge prevents nanoparticles from agglomeration (Melendrez et al., 2010). Zeta potential values within ± 30 mV limit (more positive or more negative) are considered to be stable (Mikolajczyk et al., 2015).

We demonstrated that average zeta potential values of nanoparticles were highest at -33.43 mV as described in Table 1. Highly negative (-ve) zeta potential values indicate that our ibuprofen capped AgNPs possess high stability, good colloidal nature, well-prevented aggregation and high dispersity due to negative and negative repulsions (Agnihotri et al., 2014; Kruk et al., 2015). The average particle size determined by zeta potential analyzer was up to 20 ± 1.12 nm. Mean values of zeta potential have been summarized in Table 1.

The DLS data of synthesized silver nanoparticles are depicted in Fig. S1. It is observed that the hydrodynamic size distribution and polydispersity index (PDI) showed high volume number of the maximum peaks ranging from 11.26 nm to 60.11 nm with low PDI of 0.325 (Fig. S1). The DLS analysis showed that synthesized AgNPs can be considered to be polydispersed in nature but with narrow size distribution. These results are in good agreement with the results of TEM analysis.

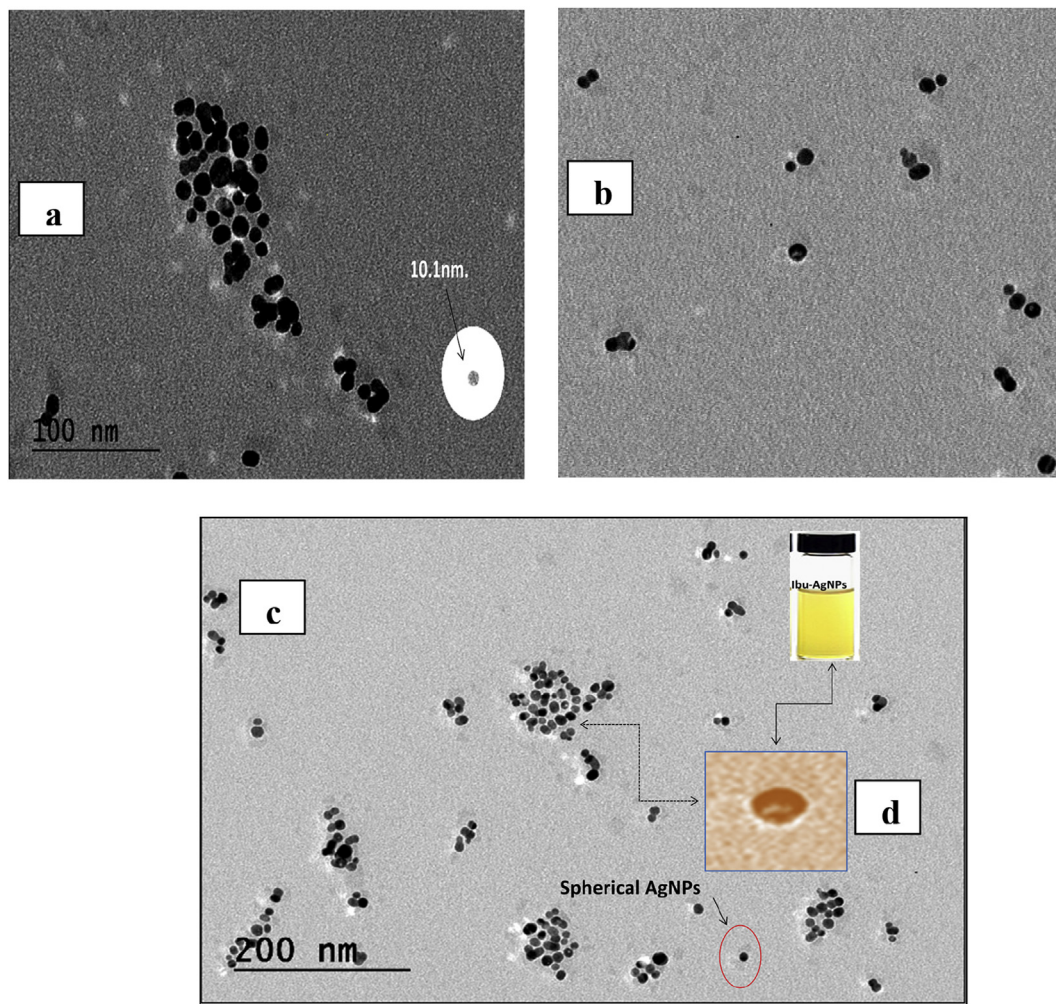


Fig. 4. TEM images of ibuprofen capped silver nanoparticles with low resolution (a,b,c) and (d) high magnification.

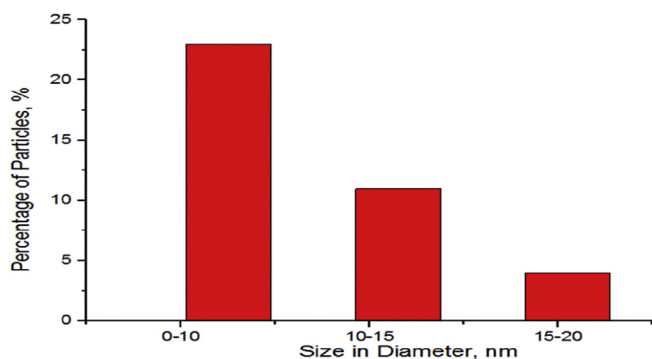


Fig. 5. TEM particle size distribution histogram of ibuprofen capped silver nanoparticles.

3.6. Ultra-fast catalytic activity of IBU-AgNPs

There are many hazardous organic compounds such as chlorophenols, nitrophenols, aromatics, cresols etc., (Dong et al., 2015; Cui et al., 2016) mainly produced by industrial activities. These pollutants are present in the environment and their potential effect on human or aquatic life is regarded as serious and threatening as these compounds have been referred as primacy toxic pollutants by the United States Environmental Protection Agency (U.S.E.P.A) (Clean Water Act, 2014). Spherical metal nanoparticles (MNPs) or core shell metal nanoparticles have high surface area to volume ratio making them better catalysts compared to bulk materials (Rajan et al., 2015; Dong et al., 2015). As reported before, MNPs can be used for the reduction of toxic nitro aromatic compounds (4-NPh) into 4-APh compounds in the presence of NaBH_4 and this activity can be monitored well with UV-Visible spectrophotometer (Sharma et al., 2007; Thakur and Thakur, 2014; Balamurugan et al., 2009).

Table 1

Summarized results of zeta potential analysis of IBU-AgNPs sol.

Sample (AgNPs)	Avg. Zeta Potential (mV)	Avg. Mobility ($\mu\text{s}/(\text{V}/\text{cm})$)	pH	Cond. (μS)	Conc. (mg/l)	Temp. ($^{\circ}\text{C}$)	Visc. (cP)	RI	Dielec. Cons.
Mean	-33.43	-2.61	5.50	31	1.00	25	0.890	1.330	78.54

Fig. 6a and b shows the peaks at 317 nm belonging to 4-NPh and at 400 nm which indicates the formation of 4-nitrophenolate ion via treatment of 4-NPh solution with NaBH₄ in the absence of AgNPs sol. In this regards, UV-visible bands at 317 nm and 400 nm clearly indicate to the presence of 4-NPh and 4-nitrophenolate ion, respectively in the absence and presence of NaBH₄ (Ma and Han, 2008) as shown in (Fig. 6a and b).

The 4-nitrophenolate ion peak at 400 nm remained unaltered with the addition of NaBH₄ solution in the absence of AgNPs sol, confirming that the reduction did not proceed by addition of NaBH₄ solution (Dong et al., 2015). 4-nitrophenolate ion is generated by the removal of a proton with the help of NaBH₄. On the other hand, 4-nitrophenolate ions can be easily and rapidly converted into 4-APh product, in the presence of the small amount of AgNPs sol (100 μL) in homogenous mixture (liquid) as a result of fast hydrogen donation process. Corresponding peak at 400 nm decreased/disappeared in a stepwise manner and new peak appearance was observed at 317 nm of (4-APh) as shown in (Fig. 7). From this behavior, the bright yellow color of solution (4-NPh) ion is altered into a colorless fashion representing due to the formation of 4-APh (Bindhu and Umadevi, 2015; Chen et al., 2006).

In this study, the AgNPs sol homogenous catalysts had adsorption sites for borohydride (BH₄⁻) ions and nitro aromatic compounds. Furthermore, the electrons transfer from BH₄⁻ ion donor to the nitro aromatic compound acceptor is supported by the catalyst (Rostami-Vartooni et al., 2016). We have succeeded in the catalytic reduction of 4-NPh into 4-APh within 40 s due to the presence of highly stable and environment friendly AgNPs sol. Ibuprofen analgesic drug molecules contain highly reactive carboxyl functional group hence they bind to Ag atoms on the nanoparticle surface with a very strong binding through carboxylate (COO⁻) sites. This fast catalytic degradation confirmed the strength of homogeneous catalysis activity of our system.

3.7. Mechanism for catalytic reduction by homogenous IBU-AgNPs sol

Scheme 2 shows the mechanism for reduction of 4-NPh into 4-APh in the presence of NaBH₄ and IBU-AgNPs homogenous catalyst. This catalytic reaction was very fast in the presence of synthesized

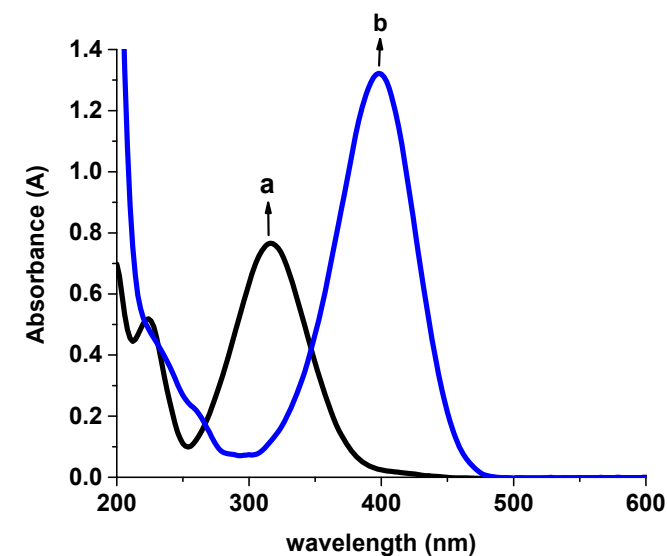


Fig. 6. (a) UV-visible spectra of 30 μM aqueous solution of 4-NP only, (b) UV-visible absorption spectra of 4-NP (30 μM) with NaBH₄ (30 mM) aqueous solution without homogenous catalyst (IBU-AgNPs).

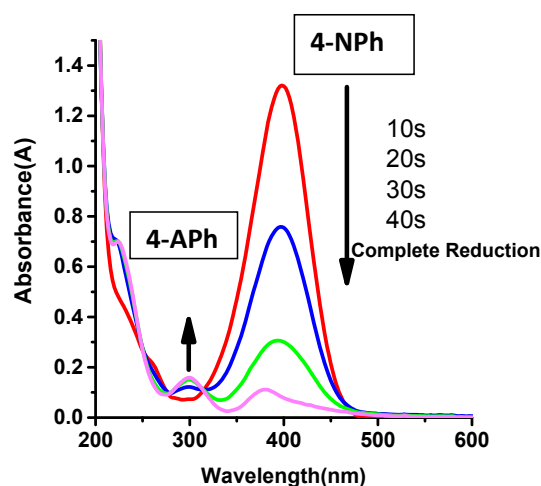
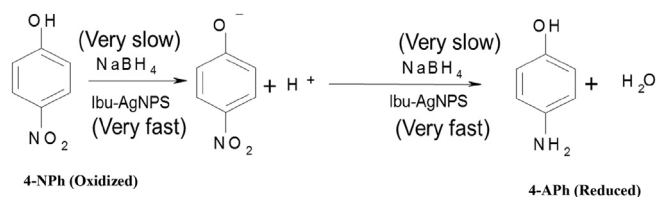


Fig. 7. UV-visible spectra of catalytic degradation of 4-NPh in the presence of 100 μL IBU-AgNPs.



Scheme 2. Mechanism for catalytic degradation of 4-NPh using IBU-AgNPs homogenous catalyst.

spherical AgNPs homogenous catalyst solution and total degradation was almost completed within 40 s. During the catalytic reaction firstly intermediate product, 4-nitrophenolate formed from 4-NPh, and then it converted into 4-APh very speedily in the presence of a small amount of AgNPs sol (100 μL) as a result of fast hydrogen transfer from NaBH₄. The peaks at 317 nm and 400 nm characteristic absorption signals of 4-NPh molecule and 4-nitrophenolate ions are shown in Fig. 7. The decrease in absorbance at 400 nm with addition of small quantity of AgNPs which acts as a fast nano-catalyst indicates to the complete reduction of 4-NPh into 4-APh. It is clearly understood that synthesized AgNPs sol with homogenous phase in catalytic system provides better access to the catalytic sites of nanoparticles as compared to the heterogeneous catalytic system (due to blockage of active sites of nanoparticles). This advantageous difference of homogenous system supports the adsorption capacity of 4-NPh on the catalyst surface and facilitates the ultra-fast reduction mechanism.

3.8. Kinetic study for catalytic reduction of 4-NPh

In order to test the validation of our data, the pseudo first order and pseudo second-order rate models were used. Fig. S2 seems the best fit between the predicted and original values in pseudo second order kinetics with r value of 0.99 and capacity factor is 10.27 μM/mL.

It is comparable to pseudo first order model with r value of 0.95 and capacity factor of 1.9 μM/mL. Calculated parameters of kinetic study are shown in Table S1.

3.9. Recovery/reuse of homogenous IBU-AgNPs catalysts

Synthesis procedure of ibuprofen capped AgNPs is simple and it

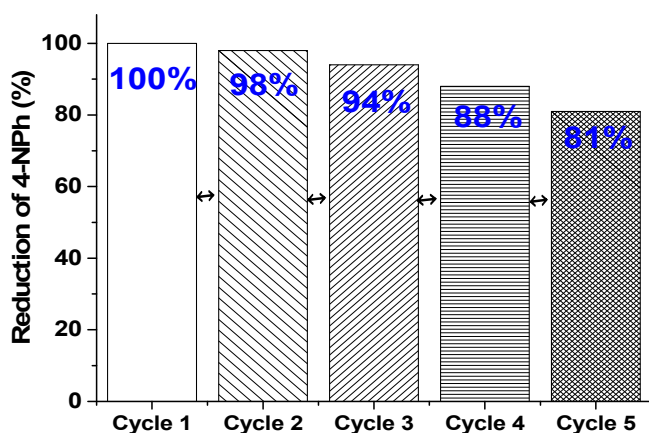


Fig. 8. Recovery/reuse of homogenous catalysts IBU-AgNPs using ionic liquid for successive five cycles with negligible loss.

is easy to use these AgNPs for catalytic reduction of toxic 4-NPh. Especially, additional advantage of simple and easy recovery and repeated reusability of homogenous AgNPs via collection on the surface of an ionic liquid is a significant contribution. A bar graph demonstrates the high catalytic efficiency of re-used homogenous AgNPs for five successive cycles from (1–5) weighted ionic liquid is shown in Fig. 8. The same NPs reduced 60 μM of 4-NPh within 40 s at each cycle. We observed negligible activity decrease for the reduction reaction after five times use due to any possible decrease or deterioration of active sites of stable, homogenous AgNPs sol at the ionic liquid surface after each cycle period. The reduction efficiency of AgNPs was obtained for reduction of 4-NPh into 4-Aph at each cycle with relative standard deviation (RSD) of 0.2, 0.6, 0.4, 0.2 and 0.5% in order of cycles respectively.

3.10. Comparisons between reported methods

Comparisons of the present study with previously reported heterogeneous and homogenous catalytic reaction system is shown in Table S2. In comparison to other reported studies, this study showed the fastest degradation rate of 4-NPh at 40 s. In heterogeneous systems, catalysis for degradation was performed on the surface of a cover glass slip. It has been suggested that this method limits catalytic activity due to adsorption of the metal nanoparticles at the glass surface, which reduces the number of active sites available to participate in catalytic reactions. Relative difference between trends is stemming from the interaction of latter metal nanoparticles with glass, probable difference of nanoparticle geometry and hence resultant selectivity (Bratlie et al., 2007). Our findings suggest that due to the higher number of accessible catalytic active sites (Burda et al., 2005), homogenous catalysts are superior to heterogeneous catalysts from selectivity, activity, high atom effectiveness and catalytic properties like regio, chemo, and stereo-selectivity are simply tuned due to fine nature of sites (Van-Klink et al., 2003). Consequently, with respect to these factors and sound observations, homogenous catalytic methods (Al-Marhaby and Seoudi, 2016) can be easier to handle and more rapid method than heterogeneous catalytic methods (Kalantari et al., 2017; Abdel-Fattah and Wixtrom, 2014; Rostami-Vartooni et al., 2016; Safari et al., 2016; Ai and Jiang, 2013) as shown in Table S2, which was considered vice versa in most cases so far.

4. Conclusions

In this study, it was concluded that ibuprofen is an efficient and

highly effective reducing and protective agent for synthesizing of AgNPs with an eco-friendly and one-pot chemical reduction method and preserving the stability thereafter. Detailed characterization was carried out by FTIR, XRD, ZP analyzer, DLS and TEM techniques to ascertain the formation of smallest size spherical, stable, well dispersed nanoparticles with average diameter of 12.5 ± 1.5 nm. The AgNPs sol proved excellent ultra-rapid homogenous catalytic activity for reductive degradation of 4-nitrophenol into 4-aminophenol in aqueous media within a very short time at 40 s under the UV-visible irradiation, due to high surface area to volume ratio. Employing a special ionic liquid recovery technique renders AgNPs advantages of easy recovery and several times of reusability without a major loss of efficiency. Use of water insoluble-room temperature ionic liquid facilitates the recovery and helps with building a greener process. In addition, recycling of AgNPs via IL method economizes the process to a greater extent and also it is proved to be time saving. Current study is expected to bring about new opportunities and solutions for treatment of many other organic hazardous compounds often present in waste water and other water resources, which incur serious impacts on environment, public health and economy due to the extendibility of this application (homogenous catalytic reductive degradation) to the degradation thereof.

Conflicts of interest

The authors declares that there is no conflict of interests.

Acknowledgments

We acknowledge the newly established US.-Pakistan Centers for Advanced studies in Water (USPCAS-W), Mehran University of Engineering and Technology (MUET) Jamshoro, Sindh Pakistan with partnering University, University of Utah, Salt Lake City, Utah, USA for providing funding and/or facilities for conducting this research.

Appendix A. Supplementary data

Supplementary data related to this article can be found at <https://doi.org/10.1016/j.envpol.2017.10.118>.

References

- Abdel-Fattah, T.M., Wixtrom, A., 2014. Catalytic reduction of 4-nitrophenol using gold nanoparticles supported on carbon nanotubes. *ECS J. Solid State Sci. Technol.* 3, M18–M20. <https://doi.org/10.1149/2.023404jss>.
- Agnihotri, S., Mukherji, S., Mukherji, S., 2014. Size-controlled silver nanoparticles synthesized over the range 5–100 nm using the same protocol and their antibacterial efficacy. *RSC Adv.* 4, 3974–3983. <https://doi.org/10.1039/c3ra44507k>.
- Ai, L., Jiang, J., 2013. Catalytic reduction of 4-nitrophenol by silver nanoparticles stabilized on environmentally benign macroscopic biopolymer hydrogel. *Bioresour. Technol.* 132, 374–377. <https://doi.org/10.1016/j.biortech.2012.10.161>.
- Aksomaitye, G., Poliakov, M., Lester, E., 2013. The production and formulation of silver nanoparticles using continuous hydrothermal synthesis. *Chem. Eng. Sci.* 85, 2–10. <https://doi.org/10.1016/j.ces.2012.05.035>.
- Al-Marhaby, F.A., Seoudi, R., 2016. Preparation and characterization of silver nanoparticles and their use in catalytic reduction of 4-Nitrophenol. *World J. Nanosci. Eng.* 6, 29–37. <https://doi.org/10.4236/wjnse.2016.61003>.
- Balamurugan, A., Ho, K.-C., Chen, S.-M., 2009. One-pot synthesis of highly stable silver nanoparticles-conducting polymer nanocomposite and its catalytic application. *Synth. Met.* 159, 2544–2549. <https://doi.org/10.1016/j.synthmet.2009.09.004>.
- Bar, H., Bhui, D.K., Sahoo, G.P., Sarkar, P., Pyne, S., Misra, A., 2009. Green synthesis of silver nanoparticles using seed extract of *Jatropha curcas*. *Colloid Surf. A* 348, 212–216. <https://doi.org/10.1016/j.colsurfa.2009.07.021>.
- Bindhu, M.R., Umadevi, M., 2015. Antibacterial and catalytic activities of green synthesized silver nanoparticles. *Spectrochim. Acta A* 135, 373–378. <https://doi.org/10.1016/j.saa.2014.07.045>.
- Bratlie, K.M., Lee, H., Komvopoulos, K., Yang, P., Somorjai, G.A., 2007. Platinum nanoparticle shape effects on benzene hydrogenation selectivity. *Nano Lett.* 7,

- 3097–3101. <https://doi.org/10.1021/nl7016000>.
- Bryaskova, R., Pencheva, D., Kyulavska, M., Bozukova, D., Debuigne, A., Detrembleur, C., 2010. Antibacterial activity of poly (vinyl alcohol)-b-poly (acrylonitrile) based micelles loaded with silver nanoparticles. *J. Colloid Interf. Sci.* 344, 424–428. <https://doi.org/10.1016/j.jcis.2009.12.040>.
- Burda, C., Chen, X., Narayanan, R., El-Sayed, M.A., 2005. Chemistry and properties of nanocrystals of different shapes. *Chem. Rev.* 105, 1025–1102. <https://doi.org/10.1021/cr030063a>.
- Chairam, S., Konkamdee, W., Parakhun, R., 2017. Starch-supported gold nanoparticles and their use in 4-nitrophenol reduction. *J. Saudi Chem. Soc.* 21, 656–663. <https://doi.org/10.1016/j.jscs.2015.11.001>.
- Chen, Y., Qiu, J., Wang, X., Xiu, J., 2006. Preparation and application of highly dispersed gold nanoparticles supported on silica for catalytic hydrogenation of aromatic nitro compounds. *J. Catal.* 242, 227–230. <https://doi.org/10.1016/j.jcat.2006.05.028>.
- Chimentao, R.J., Kirm, I., Medina, F., Rodríguez, X., Cesteros, Y., Salagre, P., Sueiras, J.E., 2004. Different morphologies of silver nanoparticles as catalysts for the selective oxidation of styrene in the gas phase. *Chem. Commun.* 0, 846–847. <https://doi.org/10.1039/b400762j>.
- Clean Water Act, 2014. Toxic and Priority Pollutants. United States Environmental Protection Agency, USA.
- Cui, X., Zuo, W., Tian, M., Dong, Z., Ma, J., 2016. Highly efficient and recyclable Ni MOF-derived N-doped magnetic mesoporous carbon-supported palladium catalysts for the hydrodechlorination of chlorophenols. *J. Mol. Catal. A-Chem.* 423, 386–392. <https://doi.org/10.1016/j.molcata.2016.07.041>.
- Darroudi, M., Zak, A.K., Muhamad, M.R., Huang, N.M., Hakimi, M., 2012. Green synthesis of colloidal silver nanoparticles by sonochemical method. *Mater. Lett.* 66, 117–120. <https://doi.org/10.1016/j.matlet.2011.08.016>.
- Dong, Z., Le, X., Dong, C., Zhang, W., Li, X., Ma, J., 2015. Ni@Pd core–shell nanoparticles modified fibrous silica nanospheres as highly efficient and recoverable catalyst for reduction of 4-nitrophenol and hydrodechlorination of 4-chlorophenol. *Appl. Catal. B-Environ.* 162, 372–380. <https://doi.org/10.1016/j.apcatb.2014.07.009>.
- Dou, X., Yuan, X., Yu, Y., Luo, Z., Yao, Q., Leong, D.T., Xie, J., 2014. Lighting up thiolated Au@Ag nanoclusters via aggregation-induced emission. *Nanoscale* 6, 157–161. <https://doi.org/10.1039/c3nr04490d>.
- Gong, J., Mullins, C.B., 2009. Surface science investigations of oxidative chemistry on gold. *Accounts Chem. Res.* 42, 1063–1073. <https://doi.org/10.1021/ar8002706>.
- Halvorson, R.A., Vikesland, P.J., 2010. Surface-enhanced Raman spectroscopy (SERS) for environmental analyses. *Environ. Sci. Technol.* 44, 7749–7755. <https://doi.org/10.1021/es101228z>.
- Hassan, S.S., Sirajuddin Solangi, A.R., Agheem, M.H., Junejo, Y., Kalwar, N.H., Tagar, Z.A., 2011. Ultra-fast catalytic reduction of dyes by ionic liquid recoverable and reusable mafenamic acid derived gold nanoparticles. *J. Hazard. Mater.* 190, 1030–1036. <https://doi.org/10.1016/j.jhazmat.2011.04.047>.
- Hassan, S.S., Sirajuddin Solangi, A.R., Kazi, T.G., Kalhor, M.S., Junejo, Y., Tagar, Z.A., Kalwar, N.H., 2012. Nafion stabilized ibuprofen–gold nanostructures modified screen printed electrode as arsenic (III) sensor. *J. Electroanal. Chem.* 682, 77–82. <https://doi.org/10.1016/j.jelechem.2012.07.006>.
- Hassan, S.S., Nafady, A., Sirajuddin Solangi, A.R., Kalhor, M.S., Abro, M.I., Sherazi, S.T.H., 2015. Ultra-trace level electrochemical sensor for methylene blue dye based on nafion stabilized ibuprofen derived gold nanoparticles. *Sens. Actuat. B-Chem.* 208, 320–326. <https://doi.org/10.1016/j.snb.2014.11.021>.
- Jagtap, U.B., Bapat, V.A., 2013. Green synthesis of silver nanoparticles using artocarpus heterophyllus lam. seed extract and its antibacterial activity. *Ind. Crop Prod.* 46, 132–137. <https://doi.org/10.1016/j.indcrop.2013.01.019>.
- Junejo, Y., Karoğlu, E., Baykal, A., Sirajuddin, 2013. Cefditorene-mediated synthesis of silver nanoparticles and its catalytic activity. *J. Inorg. Organomet. P.* 23, 970–975. <https://doi.org/10.1007/s10904-013-9882-1>.
- Junejo, Y., Sirajuddin, Baykal A., Safdar, M., Balouch, A.A., 2014. Novel green synthesis and characterization of Ag NPs with its ultra-rapid catalytic reduction of methyl green dye. *Appl. Surf. Sci.* 290, 499–503. <https://doi.org/10.1016/j.apsusc.2013.11.106>.
- Kalantari, K., Affi, A.B.M., Bayat, S., Shameli, K., Yousefi, S., Mokhtar, N., Kalantari, A., 2017. Heterogeneous catalysis in 4-nitrophenol degradation and antioxidant activities of silver nanoparticles embedded in tapioca starch. *Arab. J. Chem.* Article Number: arabjc201612018 <https://doi.org/10.1016/j.arabjc.2016.12.018>.
- Kalwar, N.H., Sirajuddin Sherazi, S.T.H., Khaskheli, A.R., Hallam, K.R., Scott, T.B., Tagar, Z.A., Hassan, S.S., Soomro, R.A., 2013. Fabrication of small L-threonine capped nickel nanoparticles and their catalytic application. *Appl. Catal. A-Gen* 453, 54–59. <https://doi.org/10.1016/j.apcata.2012.12.005>.
- Kalwar, N.H., Sirajuddin Soomro, R.A., Sherazi, S.T.H., Hallam, K.R., Khaskheli, A.R., 2014. Synthesis and characterization of highly efficient nickel nanocatalysts and their use in degradation of organic dyes. *Int. J. Metal.* 2014, 1–10. <https://doi.org/10.1155/2014/126103>.
- Kannan, P., John, S.A., 2009. Determination of nanomolar uric and ascorbic acids using enlarged gold nanoparticles modified electrode. *Anal. Biochem.* 386, 65–72. <https://doi.org/10.1016/j.ab.2008.11.043>.
- Kästner, C., Thünemann, A.F., 2016. Catalytic reduction of 4-nitrophenol using silver nanoparticles with adjustable activity. *Langmuir* 32, 7383–7391. <https://doi.org/10.1021/acs.langmuir.6b01477>.
- Khaskheli, A.R., Naz, S., Soomro, R.A., Ozul, F., Aljabour, A., Kalwar, N.H., Mahesar, A.W., Patir, I.H., Ersoz, M., 2016. L-lysine derived nickel nanoparticles for reductive degradation of organic dyes. *Adv. Mater. Lett.* 7, 616–621. <https://doi.org/10.5185/amlett.2016.6215>.
- Kiasat, A.R., Davarpanah, J., 2013. Fe₃O₄@ silica sulfuric acid nanoparticles: an efficient reusable nanomagnetic catalyst as potent solid acid for one-pot solvent-free synthesis of indazole [2, 1-b] phthalazine-triones and pyrazolo [1, 2-b] phthalazine-diones. *J. Mol. Catal. A-Chem.* 373, 46–54. <https://doi.org/10.1016/j.molcata.2013.03.003>.
- Kim, J.Y., Lee, J.S., 2010. Synthesis and thermodynamically controlled anisotropic assembly of DNA– silver nanoprisms conjugates for diagnostic applications. *Chem. Mater.* 22, 6684–6691. <https://doi.org/10.1021/cm102984m>.
- Kim, S.-E., Park, J.H., Lee, B.C., Lee, J.C., Kwon, Y.K., 2012. Large-scale synthesis of silver nanoparticles using Ag (I)–S12 polymer through electron beam irradiation. *Radiat. Phys. Chem.* 81, 978–981. <https://doi.org/10.1016/j.radphyschem.2012.02.038>.
- Klug, H.P., Alexander, L.E., 1974. *X-ray Diffraction Procedure: for Polycrystalline and Amorphous Materials*, second ed. Wiley, New York, NY, p. 992.
- Kouvaris, P., Delimitis, A., Zaspalis, V., Papadopoulos, D., Tsipas, S.A., Michailidis, N., 2012. Green synthesis and characterization of silver nanoparticles produced using arbutus unedo leaf extract. *Mater. Lett.* 76, 18–20. <https://doi.org/10.1016/j.matlet.2012.02.025>.
- Kruk, T., Szczepanowicz, K., Stefańska, J., Socha, R.P., Warszyński, P., 2015. Synthesis and antimicrobial activity of monodisperse copper nanoparticles. *Colloid Surf. B* 128, 17–22. <https://doi.org/10.1016/j.colsurfb.2015.02.009>.
- Levin, C.S., Kundu, J., Janesko, B.G., Scuseria, G.E., Raphael, R.M., Halas, N.J., 2008. Interactions of ibuprofen with hybrid lipid bilayers probed by complementary surface-enhanced vibrational spectroscopies. *J. Phys. Chem. B* 112, 14168–14175. <https://doi.org/10.1021/jp804374e>.
- Lin, D., Tian, X., Wu, F., Xing, B., 2010. Fate and transport of engineered nanomaterials in the environment. *J. Environ. Qual.* 39, 1896–1908. <https://doi.org/10.2134/jeq2009.0423>.
- Luo, Z., Nachammal, V., Zhang, B., Yan, N., Leong, D.T., Jiang, D-en, Xie, J., 2014. Toward understanding the growth mechanism: tracing all stable intermediate species from reduction of Au (I)–thiolate complexes to evolution of Au₂₅ nanoclusters. *J. Am. Chem. Soc.* 136, 10577–10580. <https://doi.org/10.1021/ja505429f>.
- Ma, Z., Han, H., 2008. One-step synthesis of cysteine-coated gold nanoparticles in aqueous solution. *Colloid Surf. A* 317, 229–233. <https://doi.org/10.1016/j.colsurfa.2007.10.018>.
- Manojkumar, K., Sivaramakrishna, A., Vijayakrishna, K., 2016. A short review on stable metal nanoparticles using ionic liquids, supported ionic liquids and poly (ionic liquids). *J. Nanopart. Res.* 18, 1–22. <https://doi.org/10.1007/s11051-016-3409-y>.
- Melendrez, M.F., Cardenas, G., Arbiol, J., 2010. Synthesis and characterization of gallium colloidal nanoparticles. *J. Colloid Interf. Sci.* 346, 279–287. <https://doi.org/10.1016/j.jcis.2009.11.069>.
- Meynen, V., Cool, P., Vansant, E.F., 2009. Verified syntheses of mesoporous materials. *Micropor. Mesopor. Mat.* 125, 170–223. <https://doi.org/10.1016/j.micromeso.2009.03.046>.
- Mikolajczyk, A., Gajewicz, A., Rasulev, B., Schaeublin, N., Gardner, E.M., Hussain, S., Leszczynski, J., Puzyn, T., 2015. Zeta potential for metal oxide nanoparticles: a predictive model developed by a nano-quantitative structure–property relationship approach. *Chem. Mat.* 27, 2400–2407. <https://doi.org/10.1021/cm504406a>.
- Mustafa, A.K., Sikka, G., Gazi, S.K., Stepan, J., Jung, S.M., Bhunia, A.K., Barodka, V.M., Gazi, F.K., Barrow, R.K., Wang, R., Amzel, L.M., Berkowitz, D.E., Snyder, S.H., Wang, R., 2011. Hydrogen sulfide as endothelium-derived hyperpolarizing factor sulfhydrylates potassium channels. *Circ. Res.* 109, 1259–1268. <https://doi.org/10.1161/circresaha.111.240242>.
- Netzer, N.L., Gunawidjaja, R., Hiemstra, M., Zhang, Q., Tsukruk, V.V., Jiang, C., 2009. Formation and optical properties of compression-induced nanoscale buckles on silver nanowires. *ACS Nano* 3, 1795–1802. <https://doi.org/10.1021/nn900419r>.
- Peng, H., Yang, A., Xiong, J., 2013. Green, microwave-assisted synthesis of silver nanoparticles using bamboo hemicelluloses and glucose in an aqueous medium. *Carbohydr. Polym.* 91, 348–355. <https://doi.org/10.1016/j.carbpol.2012.08.073>.
- Philip, D., Unni, C., Aromal, S.A., Vidhu, V.K., 2011. Murraya Koenigii leaf-assisted rapid green synthesis of silver and gold nanoparticles. *Spectrochim. Acta A* 78, 899–904. <https://doi.org/10.1016/j.saa.2010.12.060>.
- Podeh, M.R.H., Bhattacharya, S.K., Qu, M., 1995. Effects of nitrophenols on acetate utilizing methanogenic system. *Water Res.* 29, 391–399. [https://doi.org/10.1016/0043-1354\(94\)00193-B](https://doi.org/10.1016/0043-1354(94)00193-B).
- Prakash, P., Gnanaprakasam, P., Emmanuel, R., Arokiyaraj, S., Saravanan, M., 2013. Green synthesis of silver nanoparticles from leaf extract of Mimosaops elengi, Linn. for enhanced antibacterial activity against multi drug resistant clinical isolates. *Colloid Surf. B* 108, 255–259. <https://doi.org/10.1016/j.colsurfb.2013.03.017>.
- Rajan, A., Vilas, V., Philip, D., 2015. Catalytic and antioxidant properties of biogenic silver nanoparticles synthesized using areca catechu nut. *J. Mol. Liq.* 207, 231–236. <https://doi.org/10.1016/j.molliq.2015.03.023>.
- Rostami-Vartooni, A., Nasrollahzadeh, M., Alizadeh, M., 2016. Green synthesis of perlite supported silver nanoparticles using hamamelis virginiana leaf extract and investigation of its catalytic activity for the reduction of 4-nitrophenol and Congo red. *J. Alloy. Compd.* 680, 309–314. <https://doi.org/10.1016/j.jallcom.2016.04.008>.
- Safari, J., Najafabadi, A.E., Zarnegar, Z., Masoule, S.F., 2016. Catalytic performance in 4-nitrophenol reduction by Ag nanoparticles stabilized on biodegradable amphiphilic copolymers. *Green Chem. Lett. Rev.* 9, 20–26. <https://doi.org/10.1007/s11051-016-3409-y>.

- 1080/17518253.2015.1134680.
- Safdar, M., Junejo, Y., Balouch, A., 2015. Efficient degradation of organic dyes by heterogeneous cefdinir derived silver nanocatalyst. *J. Ind. Eng. Chem.* 31, 216–222. <https://doi.org/10.1016/j.jiec.2015.06.026>.
- Salam, N., Banerjee, B., Roy, A.S., Mondal, P., Roy, S., Bhaumik, A., Islam Sk, M., 2014. Silver nanoparticles embedded over mesoporous organic polymer as highly efficient and reusable nanocatalyst for the reduction of nitroarenes and aerobic oxidative esterification of alcohols. *Appl. Catal. A-Gen* 477, 184–194. <https://doi.org/10.1016/j.apcata.2014.03.014>.
- Sasidharan, M., Senthil, C., Kumari, V., Bhaumik, A., 2015. The dual role of micelles as templates and reducing agents for the fabrication of catalytically active hollow silver nanospheres. *Chem. Commun.* 51, 733–736. <https://doi.org/10.1039/c4cc07872a>.
- Sharma, N.C., Sahi, S.V., Nath, S., Parsons, J.G., Gardea-Torresdey, J.L., Pal, T., 2007. Synthesis of plant-mediated gold nanoparticles and catalytic role of biomatrix-embedded nanomaterials. *Environ. Sci. Technol.* 41, 5137–5142. <https://doi.org/10.1021/es062929a>.
- Stevanovic, M., Savanovic, I., Uskokovic, V., Skapin, S.D., Bracko, I., Jovanovic, U., Uskokovic, D., 2012. A new, simple, green, and one-pot four-component synthesis of bare and poly(α,γ -L-glutamic acid)-capped silver nanoparticles. *Colloid Polym. Sci.* 290, 221–231. <https://doi.org/10.1007/s00396-011-2540-7>.
- Tagar, Z.A., Sirajuddin, Memon N., Agheem, M.H., Junejo, Y., Hassan, S.S., Kalwar, N.H., Khattak, M.I., 2011. Selective, simple and economical lead sensor based on ibuprofen derived silver nanoparticles. *Sens. Actuat. B-Chem.* 157, 430–437. <https://doi.org/10.1016/j.snb.2011.04.082>.
- Tagar, Z.A., Sirajuddin Memon, N., Kalhor, M.S., Brien, P.O., Malik, M.A., Abro, M.I., Hassan, S.S., Kalwar, N.H., Junejo, Y., 2012. Highly sensitive, selective and stable multi-metal ions sensor based on ibuprofen capped mercury nanoparticles. *Sens. Actuat. B-Chem.* 173, 745–751. <https://doi.org/10.1016/j.snb.2012.07.093>.
- Tang, B., An, J., Zheng, X., Xu, S., Li, D., Zhou, J., Zhao, B., Xu, W., 2008. Silver nanodisks with tunable size by heat aging. *J. Phys. Chem. C* 112, 18361–18367. <https://doi.org/10.1021/jp806486f>.
- Thakur, V.K., Thakur, M.K., 2014. Recent advances in graft copolymerization and applications of chitosan: a review. *ACS Sustain. Chem. Eng.* 2, 2637–2652. <https://doi.org/10.1021/sc500634p>.
- Tsujino, K., Matsumura, M., 2005. Helical nanoholes bored in silicon by wet chemical etching using platinum nanoparticles as catalyst. *Electrochem. Solid-St. Lett.* 8, C193–C195. <https://doi.org/10.1149/1.2109347>.
- Uberoi, V., Bhattacharya, S.K., 1997. Toxicity and degradability of nitrophenols in anaerobic systems. *Water Environ. Res.* 69, 146–156. <https://doi.org/10.2175/106143097X125290>.
- Van-Klink, G.P.M., Dijkstra, H.P., Van-Koten, G., 2003. Recyclable nanosize homogeneous catalysts. *CR. Chim.* 6, 1079–1085. <https://doi.org/10.1016/j.crci.2003.07.009>.
- Wang, L., Sun, Y., Che, G., Li, Z., 2011. Self-assembled silver nanoparticle films at an air–liquid interface and their applications in SERS and electrochemistry. *Appl. Surf. Sci.* 257, 7150–7155. <https://doi.org/10.1016/j.apsusc.2011.03.077>.
- Yamamoto, M., Kashiwagi, Y., Nakamoto, M., 2006. Size-controlled synthesis of monodispersed silver nanoparticles capped by long-chain alkyl carboxylates from silver carboxylate and tertiary amine. *Langmuir* 22, 8581–8586. <https://doi.org/10.1021/la0600245>.
- Zhang, Q., Li, W., Moran, C., Zeng, J., Chen, J., Wen, L.-P., Xia, Y., 2010. Seed-mediated synthesis of Ag nanocubes with controllable edge lengths in the range of 30–200 nm and comparison of their optical properties. *J. Am. Chem. Soc.* 132, 11372–11378. <https://doi.org/10.1021/ja104931h>.